Title

Differential localization and potency of manganese porphyrin superoxide dismutase-mimicking compounds in Saccharomyces cerevisiae

Permalink

https://escholarship.org/uc/item/5rp1h5h8

Authors

Li, Alice Ma
Martins, Jake
Tovmasyan, Artak
et al.

Publication Date

2014

DOI

10.1016/j.redox.2014.09.003

Peer reviewed

Research Paper

Differential localization and potency of manganese porphyrin superoxide dismutase-mimicking compounds in *Saccharomyces cerevisiae*

Alice Ma Li [a,1], Jake Martins [a], Artak Tovmasyan [b], Joan S. Valentine [a], Ines Batinic-Haberle [b], Ivan Spasojevic [c], Edith B. Gralla [a,*]

[a] *Department of Chemistry and Biochemistry, UCLA, 607 Charles E Young Drive East, Los Angeles, CA 90095-1569, USA*
[b] *Department of Radiation Oncology, Duke University Medical Center, NC 27710, USA*
[c] *Department of Medicine and PK/PD Shared Resource of Duke Cancer Institute, Duke University Medical Center, NC 27710, USA*

ABSTRACT

Cationic Mn(III) porphyrin complexes based on MnTM-2-PyP are among the most promising superoxide dismutase (SOD) mimicking compounds being considered as potential anti-inflammatory drugs. We studied four of these active compounds in the yeast *Saccharomyces cerevisiae*, MnTM-2-PyP, MnTE-2-PyP, MnTnHex-2-PyP, and MnTnBu-2-PyP, each of which differs only in the length of its alkyl substituents. Each was active in improving the aerobic growth of yeast lacking SOD (*sod1Δ*) in complete medium, and the efficacy of each mimic was correlated with its characteristic catalytic activity. We also studied the partitioning of these compounds between mitochondria and cytosol and found that the more hydrophobic members of the series accumulated in the mitochondria. Moreover, the degree to which a mimic mitigated the *sod1Δ* auxotrophic phenotype for lysine relative to its auxotrophic phenotype for methionine depended upon its level of lipophilicity-dependent accumulation inside the mitochondria. We conclude that localization within the cell is an important factor in biological efficacy in addition to the degree of catalytic activity, and we discuss possible explanations for this effect.

Introduction

The intracellular superoxide dismutase enzymes (SODs)—copper–zinc SOD (CuZnSOD or SOD1p), found in the mitochondrial intermembrane space (IMS), cytoplasm, and nucleus, and manganese SOD (MnSOD, SOD2), found in the mitochondrial matrix—catalyze the disproportionation of superoxide to hydrogen peroxide and dioxygen. They represent a major antioxidant defense system in eukaryotic cells [1]. In the case of the budding yeast *Saccharomyces cerevisiae*, Sod1p in particular has been found to be critical for cell fitness since *sod1Δ* mutant yeast strains lacking this defense mechanism exhibit dioxygen sensitivity, poor growth in air, altered energy metabolism, and auxotrophies for lysine, methionine, and leucine [2,3]. The lysine and leucine auxotrophies are believed to result from inactivation of superoxide-sensitive iron–sulfur cluster-containing dehydratases in their biosynthetic pathways [4,5]. The enzyme homoaconitase on the biosynthetic

pathway for lysine is related to the TCA cycle enzyme aconitase; both are much decreased in activity in *sod1Δ* yeast and both are mitochondrial. The Fe–S cluster enzyme implicated in leucine auxotrophy, Leu1p, is cytoplasmic. Mutants of the fission yeast *Schizosaccharomyces pombe* that lack cytoplasmic CuZnSOD also show a lysine auxotrophy. Interestingly, in this organism the auxotrophy was attributed to inactivation of homocitrate synthase, the enzyme upstream of homoaconitase in the lysine pathway [6]. Interestingly, CuZnSOD is also involved in control of respiration rate, being part of a glucose repression pathway that reduces respiration even in the presence of oxygen [7].

Alterations in superoxide metabolism have been linked to a large variety of human pathologies, including accelerated aging and neurodegenerative disease [8,9], leading to an interest in development of drugs that could provide protection against the effects of elevated oxidative stress. A variety of SOD-mimicking compounds have been developed and explored for their effectiveness in treating oxidative stress-related pathologies [10,11]. One of the most promising classes of these potential drugs is a series of cationic Mn(III) porphyrins (MnPs, [12]). The most effective SOD mimics in this class (Diagram 1) have the *meso* positions of their porphyrin rings substituted with *ortho-N*-alkylpyridinium substituents [13,14].
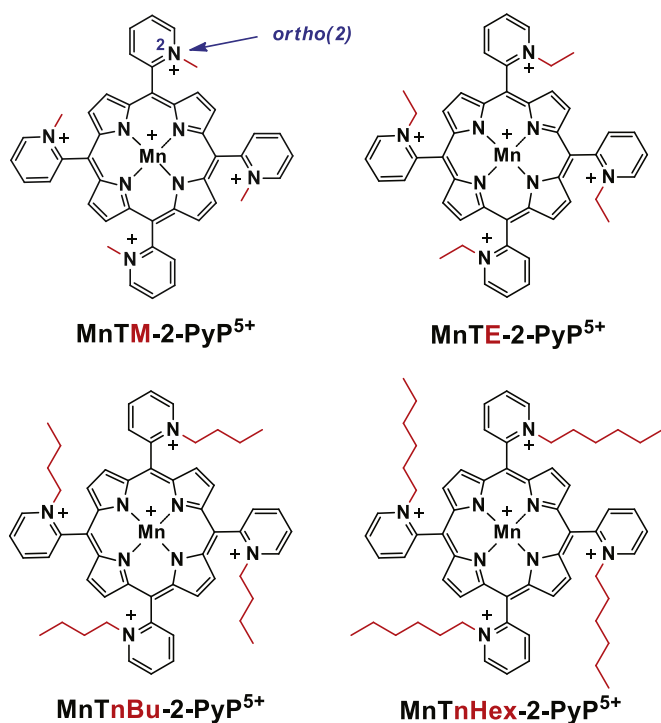
Fig. 1. The structures of Mn(III) porphyrin-based SOD mimics.

Substitution at the *ortho* position with positively charged pyridyl nitrogens was chosen to adjust thermodynamic and kinetics for the $O_2^{\cdot-}$ dismutation and to hinder the planar MnP ring sterically from interacting substantially with DNA and RNA, thereby improving its catalytic efficiency *in vivo*.

A survey in yeast and *Escherichia coli* comparing the biological activities of several diverse SOD mimics of different classes found that only the cationic Mn porphyrins could substitute for the bona fide SOD enzyme and facilitate the aerobic growth of yeast lacking CuZnSOD (*sod1Δ*) [15]. The two compounds of that class used in that study were MnTM-2-PyP^{5+} and MnTE-2-PyP^{5+}, both cationic MnPs with *ortho* N-alkylpyridinium groups substituted at the *meso* positions (see Fig. 1). Both compounds demonstrated considerable capacity to restore *sod1Δ* growth under aerobic conditions. Specifically, Mn-TM2-PyP restored growth in air to wild type levels, even in media lacking methionine or lysine in which the *sod1Δ* strain does not normally grow at all.

In the current study, we explore four of the cationic MnP-based SOD mimics in this series that differ only in the length of the substituents at the *ortho* position. The N-alkylpyridinium groups for each compound differ according to whether methyl-(MnT**M**-2-PyP^{5+}), ethyl-(MnT**E**-2-PyP^{5+}), n-butyl-(MnT**nBu**-2-PyP^{5+}), or n-hexyl-(MnT**nHex**-2-PyP^{5+}) hydrocarbon chain ends have been attached to the four pyridyls (Fig. 1). The larger N-alkyl groups enhance the lipophilicity and thus the ability of the Mn porphyrin, which carries overall positive charge, to penetrate cell membranes. The compound's lipophilicity influences both its intracellular availability and the range of concentrations over which it improves the growth of SOD-deficient bacteria and/or inhibits the growth of SOD-replete bacteria [14,16]. Our results indicate that each of these four MnP-based mimics indeed provides beneficial effects to the growth of *sod1Δ* yeast in an aerobic environment and that the potency in substituting for the SOD enzyme depends largely on its characteristic catalytic activity. We find further that the increasing lipophilicity of a mimic correlates positively with its degree of localization to the mitochondria relative to the cytosol, and that this localization influences the capacity of a mimic to mitigate the lysine relative to the methionine auxotroph of *sod1Δ* yeast.

Methods

Yeast strains and pre-culture conditions

The wild-type *S. cerevisiae* strain used was EG103, (*MATα, leu2, his3, trp1, ura3*). The *sod1Δ* mutant strain was EG118, (*MATα, leu2, his3, trp1, ura3, sod1Δ::URA3*) was derived from it by gene replacement [17]. For growth experiments cells were first streaked from 20% glycerol stocks onto yeast extract, peptone, 2% dextrose agar (YPD) [18] and incubated for 72 h at 30 °C under conditions of low oxygen. Single colonies were then selected to grow overnight at 30 °C in synthetic complete liquid medium supplemented with 2% dextrose (SDC) as described [17]. All synthetic dextrose (SD) liquid media were adjusted to pH 6.0 unless otherwise noted.

Growth experiments

Growth of the yeast cells was measured using cultures' absorbance (optical density) at 600 nm (A_{600} or OD_{600}; a value of 1 is equivalent to 1×10^7 cells/mL). Cells from overnight pre-cultures were inoculated into 10 mL of liquid SDC, SD-Lys, or SD-Met (specific amino acids that were omitted from media are indicated) in 50 mL flasks at an initial OD_{600} of 0.05 and grown at 30 °C, shaking at 220 rpm under aerobic conditions. All media were treated with MnP concentrations as indicated. Error bars denote standard deviations.

Manganese porphyrin SOD mimics

MnTE-2-PyP^{5+}, MnTM-2-PyP^{5+}, MnTnHex-2-PyP^{5+}, and MnTnBu-2-PyP^{5+} (Fig. 1), were synthesized as described [13], and filter sterilized with a 0.22 µm filter (Whatman, Middlesex, UK) before utilization in experimental procedures.

Toxicity assay procedure

Wild-type yeast cells from overnight pre-cultures were inoculated at 0.05 OD_{600} into 10 mL SDC pH 6.0 in 50 mL flasks and incubated at 220 rpm, 30 °C until they reached an OD_{600} of 0.5–2 (log phase). The cells were then spun down, washed with water, and resuspended at 0.1 OD_{600} in glass tubes containing 0.5 mL water or SDC with varying concentrations of SOD mimics. Cells were aerobically incubated under these conditions for 1–2 h before being diluted and plated onto YPD agar, on which they were allowed to grow for 48 h.

Mitochondrial and cytosolic isolation procedure

Wild-type yeast cells from overnight pre-cultures were inoculated at 0.1 OD_{600} into 500 mL SDC pH 6.0 containing the indicated MnP at 10 µM. After growing at 220 rpm at 30 °C under aerobic conditions in this medium for 18–24 h, the cells were harvested and spun down for 5 min at 3500 rpm. Mitochondria were isolated as described by [19]. During this mitochondrial purification process, cytosolic fractions of the wild-type yeast were collected from supernatants immediately after the first 10 min, 10,000 rpm pelleting step.

Measurements of manganese porphyrin SOD mimic using liquid chromatography electrospray ionization tandem mass spectrometry (LC/ESI-MS/MS)

Measurements were performed in PK/PD Shared Resource of Duke Cancer Institute. Samples to be measured were first prepared by adding 25 µL of cytosol or mitochondrial homogenate, 25 µL of water, and 5 µL of 5 µM internal standard solution in water (see

MS/MS conditions below) to a 2 mL polypropylene screw-cap vial. After letting this mixture stand at room temperature for 10 min, 100 μL of 1% acetic acid in methanol was added. Next, the sample was vigorously mixed (Fast Prep, 40 s, speed 6) and left at −20 °C for 15 min. The sample was then centrifuged at 16,000g at 4 °C for 15 min. To prepare sample for injection into LC/MS/MS system, 100 μL of supernatant was pipetted into 5 mL-polypropylene round-bottom tube, which was placed in rotary evaporator (Speed Vac) at 50 °C for 1 h. Residue remaining after evaporation was dissolved in 100 μL mobile phase A (see LC conditions below), spun for 5 min at 16,000g in 4 °C. Of this final mixture, 20 μL was injected into LC/MS/MS system.

LC conditions

A Shimadzu 20A series high pressure liquid chromatography system (HPLC) was used, with a Phenomenex 4×3 mm^2 C18 guard cartridge analytical column. The column temperature was maintained at 35 °C. Mobile phase A was 5% acetonitrile and 0.0005% heptafluorobutyric acid, HFBA. Mobile phase B was acetonitrile, which had the following elution gradient: 0–0.2 min 0–90% B, 0.2–0.7 min 90% B, 0.7–0.75 min 90–100% B. Run time was 4 min.

MS/MS conditions

The mass spectrometer used was Applied Biosystems MDS Sciex 3200 Q Trap or 4000 Q Trap ESI-MS/MS. MRM transitions observed were as follows (parent ion $[MnP^{5+} + 3HFBA -]2 + /2$):

| Analyte	Internal standard
MnTM-2-PyP^{5+}, m/z 685.3/ 356.6	MnTE-2-PyP^{5+}, m/z 713.3/ 363.6
MnTE-2-PyP^{5+}, m/z 713.3/ 363.6	MnTM-2-PyP^{5+}, m/z 685.3/ 356.6
MnTBu-2-PyP^{5+}, m/z 769.3/ 398.8	MnTnHex-2-PyP^{5+}, m/z 825.5/ 611.5
MnTnHex-2-PyP^{5+}, m/z 825.5/611.5	MnTnHep-2-PyP^{5+}, m/z 853.5/ 639.5.

Sample calibrations, in which known amounts of pure analytes are mixed with cellular homogenates and analyzed in conjunction with experimental samples, occurred in the 1–300 nM or 0.1–30 μM range. For the concentrations used, a linear response was observed.

A Bradford Protein Assay Kit (Bio-Rad) was used to determine the protein concentrations, which were used to normalize the Mn porphyrin mimic concentrations determined using HPLC.

Results

In this study, we first assessed the potency of the new Mn porphyrins by examining their effects on the aerobic growth of *sod1Δ S. cerevisiae*. In a previous study [15], it was shown that MnTM-2-PyP^{5+} and MnTE-2-PyP^{5+} significantly improved the growth of *sod1Δ* yeast in SDC. We now extend these data to include MnTnBu-2-PyP^{5+} and MnTnHex-2-PyP^{5+}. Fig. 2 shows that the new compounds improve growth of *sod1Δ* yeast in synthetic complete medium (SDC) to approximately the same extent as MnTE-2-PyP^{5+}.

To explore further the relative efficacy of these Mn porphyrin mimics *in vivo*, we tested their ability to improve the growth of *sod1Δ* yeast in medium lacking lysine or methionine (SD-Lys or SD-Met). These conditions are far more stringent, as *sod1Δ* yeast show little or no growth in these media. The data presented in
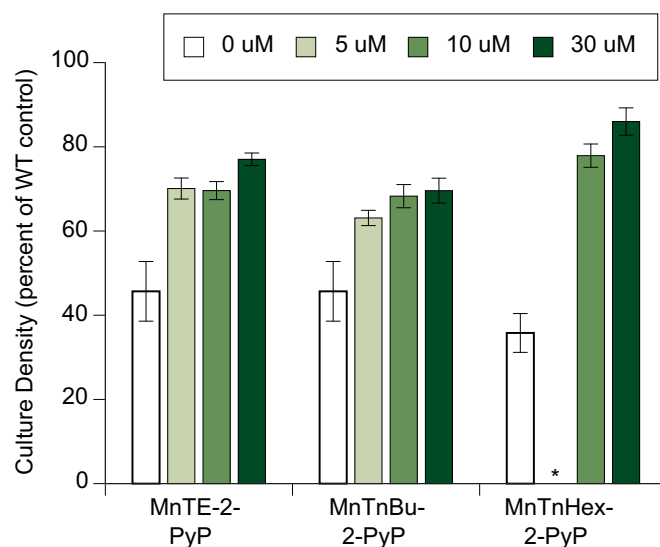
Fig. 2. Effect of Mn TE-2-PyP^{5+}, MnTnBu-2-PyP^{5+} and MnTnHex-2-PyP^{5+} on growth of *sod1Δ* yeast under aerobic conditions. Cultures were grown for 24 h at 30 °C, shaking at 220 rpm in SDC with mimic concentrations as indicated. Cell density was measured using turbidity of cultures at 600 nm. The values presented are averages of three independent yeast cultures grown on the same day, with error bars signifying standard deviation. Student 2-tailed *T*-tests were performed; the difference between control and each experimental point was significant ($P < 0.05$). Representative experiments are shown (* not tested.).

Fig. 3 showed that both MnTnHex-2-PyP^{5+} and MnTE-2-PyP^{5+} consistently rescued the growth of the *sod1Δ* in SD-Lys significantly more than in SD-Met. In contrast, MnTM-2-PyP^{5+} and MnTnBu-2-PyP^{5+} restored the growth of these mutant yeast auxotrophic phenotypes to the same extent in both media, although the TM compound was far more effective in both.

The methionine-synthesizing pathway uses a large amount of NADPH, and its sensitivity to superoxide stress is believed to be due to depletion of NADPH in the cytosol in *sod1Δ* yeast [20]. On
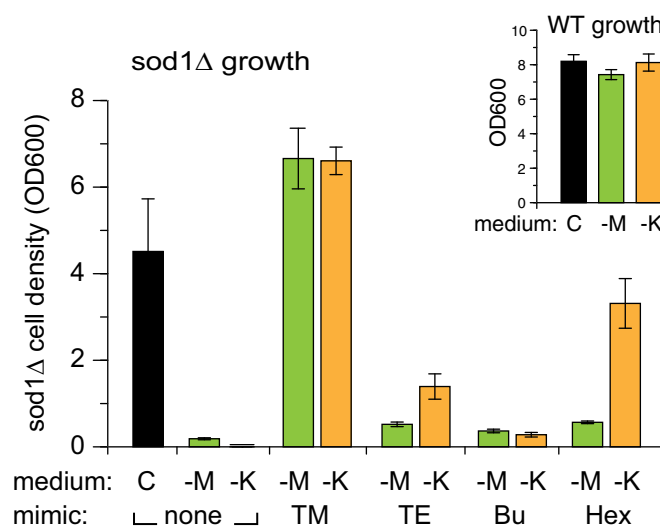
Fig. 3. *sod1Δ S. cerevisiae* aerobic growth in SD-Met (-M, green bars), SD-Lys (-K, orange bars) or SD-complete (C, black bars). Cells were inoculated at low density, treated (or not) with 30 μM MnTM-2-PyP^{5+} (TM), MnTE-2-PyP^{5+} (TE), MnTnBu-2-PyP^{5+} (Bu), or MnTnHex-2-PyP^{5+} (Hex), and incubated at 30 °C and 220 rpm for 24 h, after which cell density was determined. Values shown are the averages calculated from three independent colonies, with error bars representing standard deviation. Student 2-tailed *T*-tests were performed. There is no significant difference between WT growth (inset) in the three media. For *sod1Δ*, the differences are significant ($P < 0.05$) between complete and drop out media; between treated and no mimic samples in all cases; and between samples grown in -Met and -Lys in the case of TE and Hex.
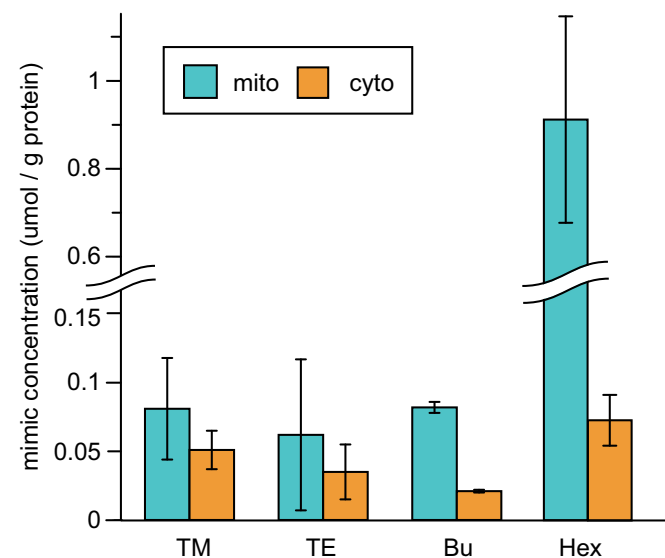
the other hand, the lysine auxotrophy in *sod1Δ* yeast is due to inactivation of homoaconitase, a superoxide-sensitive 4Fe–4S cluster enzyme found in the mitochondrial matrix [5]. In light of these previous findings, we wondered whether MnTE-2-PyP^{5+} and especially MnTnHex-2-PyP^{5+} were localizing to the mitochondria while the other compounds were more evenly distributed between the mitochondrial and cytosolic compartments. If so, this could explain the observed differences in levels of rescue exerted by the mimics upon the growth of *sod1Δ* yeast in SD-Lys and SD-Met. Since the MnTnHex-2-PyP^{5+} was designed to be more lipophilic, this experiment would also show that its design had the same intended consequences.

To test this hypothesis, we isolated cytosolic and mitochondrial fractions from wild-type yeast cells treated with 10 μM MnTM-2-PyP^{5+} MnTE-2-PyP^{5+}, MnTnBu-2-PyP^{5+} or MnTnHex-2-PyP^{5+} and measured the concentrations of these compounds in each fraction. The values obtained were normalized to the protein concentration in the sample. The results in Fig. 4 show that MnTnHex-2-PyP^{5+} exhibits a very strong preference for a mitochondrial location, MnTnBu-2-PyP^{5+} shows a moderate preference, while MnTM-2-PyP^{5+}, MnTE-2-PyP^{5+} are more evenly distributed.
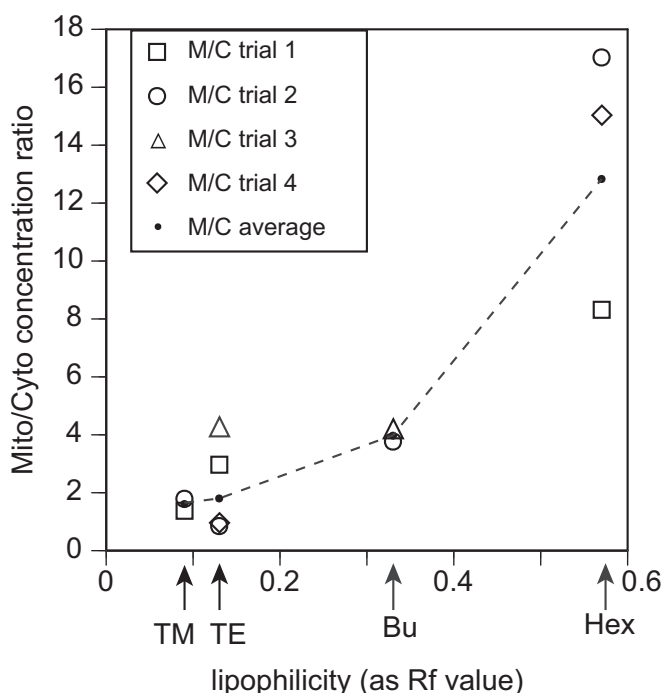
Further analysis of our measurements indicated that the degree of mitochondrial localization of each Mn porphyrin mimic roughly correlates with known measurements of its overall lipophilicity, or thin layer chromatography R_f value [14,16] in Fig. 5.

Thus, we see an overall positive correlation between lipophilicity and mitochondrial localization in our data, but it is not linear (at least in this method of plotting). MnTnHex-2-PyP^{5+} localizes far more strongly to the mitochondria than the others, and there is some discrepancy between the relative activities of each in the auxotrophy rescue assays (see Discussion section).

The toxicity of these mimics has been an issue in other systems. For example, *E. coli* treated with MnTnHex-2-PyP^{5+} did not grow in liquid cultures unless the concentration was substantially reduced [16]. We noted no such effect on liquid cultures of yeast,

Fig. 5. Degree of mitochondrial localization of Mn porphyrin mimic *vs.* compound lipophilicity (denoted by R_f value) for four trials. Wild-type *S. cerevisiae* treated with the four mimic compounds were grown as described in Fig. 3. The degree of mitochondrial localization was calculated by dividing the Mn porphyrin mimic concentration to protein concentration ratio of the mitochondrial fraction by that of the cytosolic fraction from wild-type yeast cells treated with the indicated Mn porphyrin mimic for each trial. (Trials are indicated in the legend.) The R_f values were taken from [14,21].

but, in order to determine whether the compounds had any toxicity in yeast, a more stringent plated colony formation assay was performed. Wild type and *sod1Δ* yeast were treated with the series of mimics for an hour and then washed, spread on YPD plates and grown in air. After 24 h colonies were counted. Only the most lipophilic mimic, MnTnHex-2-PyP^{5+} showed any inhibition of colony formation (Fig. 6), and that inhibition was far from complete, especially for the *sod1Δ* strain. We do not understand why the WT strain seems to be more sensitive than the *sod1Δ* strain to MnTnHex-2-PyP^{5+}. One possibility is that the higher mitochondrial number and increased reliance on respiration that is observed in *sod1Δ* strains during glucose growth [3] could make them more resistant to this compound, which heavily accumulates in mitochondria. It should be noted that if the 1-h drug treatment was carried out in water rather than liquid growth medium the compounds were far more toxic (data not shown).

Discussion

In this paper we examined the biological efficacy of a series of manganese porphyrin-based SOD mimics of increasing lipophilicity, and we related their effectiveness to their tendency to localize to the mitochondria *vs.* the cytoplasm. It should be noted that this is the only study to date that (1) examines both cytosolic and mitochondrial concentrations a logically graduated series of mimics from the same samples and that (2) relates this localization to the mimic's ability to replace the biological activity of SOD1 in yeast lacking this protein.

Direct measurements of the specific concentrations of these compounds inside the mitochondria and cytosol of yeast cells were performed. We demonstrated that the degree of the mitochondrial localization of a mimic correlates with its overall

Fig. 4. Distribution of Mn porphyrin mimic in mitochondria (aqua bars) and cytosol (orange bars) isolated from wild-type *S. cerevisiae* grown in SDC for 24 h at 220 rpm in 30 °C with 10 μM MnTM-2-PyP^{5+} (TM), MnTE-2-PyP^{5+} (TE), MnTnBu-2-PyP^{5+} (Bu), or MnTnHex-2-PyP^{5+} (Hex). Each mimic distribution value displayed was determined using measurements from at least two trials, with error bars representing standard deviation. Concentrations of the Mn porphyrin mimics were measured using high-pressure liquid chromatography and then normalized to protein concentrations determined *via* Bradford assays in the respective mitochondrial and cytosolic fractions. Student 2-tailed *T*-tests were performed; the difference between mitochondrial and cytosolic concentration was significant ($P < 0.05$) in the cases of Bu and hex only.
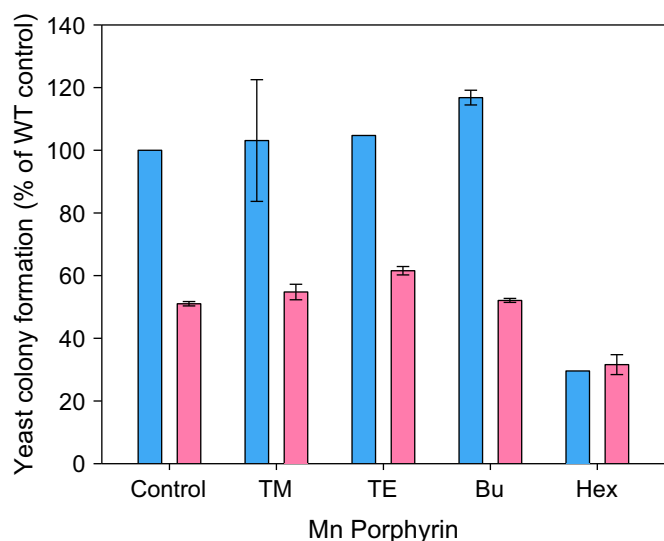
Fig. 6. Plated toxicity assay examining effects of SOD mimic at 30 µM on colony formation for WT (black bars) and *sod1Δ* yeast (gray bars). Cells were treated with 30 µM of the indicated SOD mimic in SDC for 1 h and then placed on YPD plates. Control samples had no mimic. Values shown are the averages of the percentages calculated from two independent cultures (with exception of WT treated with MnTnHex-2-PyP^{5+} and MnTE-2-PyP^{5+}, for which there was only one culture in this experiment). Percentage colony formation, relative to WT untreated control is shown. Student 2-tailed *T*-tests were performed. The difference between control and treated samples was not significant ($P < 0.05$) except in the case of Hex.

lipophilicity (Fig. 5). That is, the higher the lipophilicity, the higher the concentration of mimic within mitochondria, as compared to the cytosol. The most lipophilic mimic in fact showed a startlingly high mitochondrial to cytoplasmic ratio.

The relationship of lipophilicity to biological efficacy is more complex. The bioavailability of SOD mimics is important in determining their therapeutic significance and can be affected by biological factors, including, uptake, intracellular transport mechanisms and final localization. In our hands, the least lipophilic compound in our series, MnTM-2-PyP^{5+}, was the most effective, fully rescuing growth in either SD-Met and SD-Lys, while the third in the series, MnTnBu-2-PyP, was the least effective, barely rescuing in either medium. The second and fourth members of the series, MnTE-2-PyP^{5+} and MnTnHex-2-PyP^{5+}, were intermediate in effectiveness (Fig. 3).

The biological activity of MnTnBu-2-PyP^{5+} was unexpectedly low, and there are two factors that may help explain these results. First, the intrinsic (*in vitro*) activity level of MnTnBu-2-PyP^{5+} is lower than that of MnTnHex-2-PyP^{5+}, MnTM-2-PyP^{5+}, or MnTE-2-PyP^{5+} [14]. This lower activity is proposed to result from unfavorable steric effects due to the n-butyl pyridyl substituents. The longer, more hydrophobic alkyl chains of MnTnHex-2-PyP^{5+} are proposed to desolvate the metal center in a way that increases the redox potential and overcomes the unfavorable steric effects, increasing its activity [13]. Second, we found that the cellular concentration, especially in the cytoplasm, was low (Fig. 4). This difference may be due to differences in the way the different compounds interact with biological transporters, membranes, and pores. For example, MnTM-2-PyP^{5+} may be small enough to be taken up through a pore for charged compounds, while MnTnHex-2-PyP^{5+} may be lipophilic enough to slip in through the membrane (or indeed remain in the membrane). MnTnBu-2-PyP^{5+} may be too big for that pore but still too charged to easily enter the lipid bilayer, potentially explaining its reduced accumulation and activity.

Each of the mimics restored growth of *sod1Δ* strains in liquid complete medium to close to wild type levels (Fig. 2 and [15]). When the more stringent tests of growth without lysine or methionine (amino acid auxotrophies) are applied, efficacy did

not fully follow lipophilicity. Because we can distinguish mitochondrial from cytosolic effects functionally *via* the differential rescue of the methionine and lysine auxotrophies, we can gain further insight.

Interestingly, if we compare the lysine auxotrophy rescue by MnTE-2-PyP^{5+} with that by MnTnHex-2-PyP^{5+}, we can conclude that the large accumulation of MnTnHex-2-PyP^{5+} inside the mitochondria renders it far better at rescuing the lysine auxotrophy than MnTE-2-PyP^{5+}. Thus this result supports the idea that the lysine auxotrophy is mitochondrially based and suggests that cell protection can be effectively enhanced by targeting SOD mimics to the mitochondria to increase localized antioxidant activity.

We previously proposed that the lysine auxotrophy of *sod1Δ* yeast is due to inhibition of homoaconitase in mitochondria of *sod1Δ* yeast. Homoaconitase contains exposed iron–sulfur clusters, which are very sensitive to oxidation by superoxide, and its activity is strongly reduced in *sod1Δ* strains of yeast [5]. However, this may not be the whole story. The rather complex regulation of the early parts of the lysine biosynthetic pathway are carried out in the nucleus and mitochondria. In *S. pombe*, the lysine auxotrophy in strains lacking CuZnSOD appears to be due to inactivation of homocitrate synthase [6]. While this inactivation has not been observed in *S. cerevisiae*, overexpression of the same enzyme (which in *S. cerevisiae* is coded for by the nearly identical lys20 and lys21 genes and is found in the nucleus) improves growth of *sod1Δ* strains in medium lacking lysine [4]. Iron metabolism may play a role as well. *Sod1Δ* yeast have an increased iron demand, turn on high affinity iron transport [22], and accumulate an oxidized form of EPR-detectable "free iron" which is not thought to be bioavailable [23]. Thus it is possible, or even likely, that the *sod1Δ* mutation triggers an iron-sparing program, for which aconitase and homoaconitase would be logical targets.

Lysine biosynthesis is also influenced by retrograde signaling through the RTG pathway, which senses respiratory dysfunction in the mitochondria and alters nuclear gene expression to maintain the supply of biosynthetic intermediates (*e.g.* alpha ketogluterate, glutamine) and lysine. Under normal conditions, MKS1 functions as an inhibitor of the RTG pathway ([24], reviewed in [25]). Constitutive induction of the RTG pathway through mutations in MKS1 has been shown to relieve the aerobic lysine auxotrophy of *sod1Δ* strains, indicating a possible involvement of this pathway [26]. (The role of this pathway in explaining the mimic effects is questionable, however, since if the *sod1Δ* mutation induced the RTG pathway it should bypass the lysine auxotrophy.) In any case, each of these mechanisms plays out in the mitochondria, so the increased localization of the Hex compound to the mitochondria can explain its preferential rescue of the lysine auxotrophy.

The generally accepted explanation for the methionine auxotrophy of *sod1Δ* yeast is that it is due to a cytosolic shortage of reducing equivalents in the form of NADPH, which are required to synthesize methionine [20]. Thus, overexpression of *ZWF1* (G6PDH, which catalyzes the first step in the pentose phosphate pathway) improves growth of *sod1Δ* strains by increasing flux through that pathway, resulting in increased NADPH generation. Furthermore, work by the Bilinski laboratory [27] supports this mechanism by showing that the methionine auxotrophy is better rescued than the lysine auxotrophy by redox-active agents such as cysteine, glutathione, *N*-acetyl cysteine and ascorbate, which are orders of magnitude less strong superoxide scavengers than SOD but do accumulate in the cytosol and feed into the supply of cellular reducing power. Our results with MnTM-2-PyP^{5+} and MnTE-2-PyP^{5+} that both accumulate in the cytosol fit well with this mechanism.

MnTnHex-2-PyP^{5+} and the even more lipophilic MnTnOct-2-PyP^{5+} were reported to be quite toxic to SOD-replete and SOD-deficient *E. coli* [14,16], inhibiting growth at concentrations

above 1 μM. While yeast are more resistant, these experimental findings are consistent with our toxicity assay results which showed that MnTnHex-2-PyP^{5+} inhibits colony [28] formation of wild type yeast and *sod1Δ* yeast (Fig. 6). The observed effects on *E. coli* were suggested to result from the compounds acting as detergents inside the cells, something that could occur in mitochondria as well.

Our results in yeast agree well with findings in mice. First, in pharmaco-kinetic studies, MnTnHex-2-PyP^{5+} showed much better tissue penetration and retention than MnTE-2-PyP^{5+}, due to its higher lipophilicity [28]. In addition, biological activity was shown when a related Mn porphyrin (MnTnBuOE-2-PyP^{5+}) was found to reduce the cardiac toxicity of the redox active drug Doxorubicin [29] and to substitute for the mitochondrial enzyme MnSOD in MnSOD knock-down mice [30].

Overall, our results indicate that subcellular localization plays an important role in determining the efficacy of SOD mimicking drugs against particular targets and that increasing lipophilicity can direct such compounds to the mitochondria. Along with increasing our understanding of superoxide toxicity in yeast, these results may help direct development of more effective redox therapeutics for humans.

Acknowledgments

References

[1] Y. Sheng, I.A. Abreu, D.E. Cabelli, M.J. Maroney, A.F. Miller, M. Teixeira, J.S. Valentine, Superoxide dismutases and superoxide reductases, Chemical Reviews 114 (2014) 3854–3918. http://dx.doi.org/10.1021/cr4005296 24684599.

[2] E.B. Gralla, Superoxide dismutase: studies in the yeast *Saccharomyces cerevisiae*, in: J.G. Scandalios (Ed.), Oxidative Stress and the Molecular Biology of Antioxidant Defenses, Cold Spring Harbor Laboratory Press, Cold Spring Harbor, NY, 1997, pp. 495–525.

[3] S. Sehati, M.H. Clement, J. Martins, L. Xu, V.D. Longo, J.S. Valentine, E.B. Gralla, Metabolic alterations in yeast lacking copper–zinc superoxide dismutase, Free Radical Biology & Medicine 50 (2011) 1591–1598. http://dx.doi.org/10.1016/j.freeradbiomed.2011.03.004 21397007.

[4] M.H. Clement, Uncovering targets of superoxide in the budding yeast *Saccharomyces cerevisiae* (doctoral dissertation), UCLA, 2008.

[5] M.A. Wallace, L.L. Liou, J. Martins, M.H. Clement, S. Bailey, V.D. Longo, J.S. Valentine, E.B. Gralla, Superoxide inhibits 4Fe–4S cluster enzymes involved in amino acid biosynthesis. Cross-compartment protection by CuZn-superoxide dismutase, Journal of Biological Chemistry 279 (2004) 32055–32062. http://dx.doi.org/10.1074/jbc.M403590200 15166213.

[6] E.S. Kwon, J.H. Jeong, J.H. Roe, Inactivation of homocitrate synthase causes lysine auxotrophy in copper/zinc-containing superoxide dismutase-deficient yeast Schizosaccharomyces pombe, Journal of Biological Chemistry 281 (2006) 1345–1351. http://dx.doi.org/10.1074/jbc.M506611200 16299000.

[7] A.R. Reddi, V.C. Culotta, SOD1 integrates signals from oxygen and glucose to repress respiration, Cell 152 (2013) 224–235. http://dx.doi.org/10.1016/j.cell.2012.11.046 23332757.

[8] T. Fukai, M. Ushio-Fukai, Superoxide dismutases: role in redox signaling, vascular function, and diseases, Antioxidants & Redox Signaling 15 (2011) 1583–1606. http://dx.doi.org/10.1089/ars.2011.3999 21473702.

[9] B. Halliwell, J.M.C. Gutteridge, Free Radicals in Biology and Medicine, Oxford University Press, New York, NY., 2007.

[10] I. Batinic-Haberle, A. Tovmasyan, E.R. Roberts, Z. Vujaskovic, K.W. Leong, I. Spasojevic, SOD therapeutics: latest insights into their structure–activity relationships and impact on the cellular redox-based signaling pathways, Antioxidants & Redox Signaling 20 (2014) 2372–2415. http://dx.doi.org/10.1089/ars.2012.5147 23875805.

[11] I. Batinic-Haberle, I. Spasojevic, Complex chemistry and biology of redox-active compounds, commonly known as SOD mimics, affect their therapeutic effects, Antioxidants & Redox Signaling 20 (2014) 2323–2325. http://dx.doi.org/10.1089/ars.2014.5921 24650329.

[12] A. Tovmasyan, H. Sheng, T. Weitner, A. Arulpragasam, M. Lu, D.S. Warner, Z. Vujaskovic, I. Spasojevic, I. Batinic-Haberle, Design, mechanism of action, bioavailability and therapeutic effects of mn porphyrin-based redox modulators, Medical Principles and Practice: International Journal of the Kuwait University, Health Science Centre 22 (2013) 103–130. http://dx.doi.org/10.1159/000341715 23075911.

[13] I. Batinić-Haberle, Manganese porphyrins and related compounds as mimics of superoxide dismutase, Methods in Enzymology 349 (2002) 223–233 11912911.

[14] A. Okado-Matsumoto, I. Batinić-Haberle, I. Fridovich, Complementation of SOD-deficient *Escherichia coli* by manganese porphyrin mimics of superoxide dismutase activity, Free Radical Biology & Medicine 37 (2004) 401–410. http://dx.doi.org/10.1016/j.freeradbiomed.2004.04.040 15223074.

[15] W. Munroe, C. Kingsley, A. Durazo, E.B. Gralla, J.A. Imlay, C. Srinivasan, J.S. Valentine, Only one of a wide assortment of manganese-containing SOD mimicking compounds rescues the slow aerobic growth phenotypes of both *Escherichia coli* and *Saccharomyces cerevisiae* strains lacking superoxide dismutase enzymes, Journal of Inorganic Biochemistry 101 (2007) 1875–1882. http://dx.doi.org/10.1016/j.jinorgbio.2007.07.008 17723242.

[16] A. Tovmasyan, J.S. Rebouças, L. Benov, Simple biological systems for assessing the activity of superoxide dismutase mimics, Antioxidants & Redox Signaling 20 (2014) 2416–2436. http://dx.doi.org/10.1089/ars.2013.5576 23964890.

[17] E.B. Gralla, J.S. Valentine, Null mutants of *Saccharomyces cerevisiae* Cu,Zn superoxide dismutase: characterization and spontaneous mutation rates, Journal of Bacteriology 173 (1991) 5918–5920 1885557.

[18] C. Kaiser, S. Michaelis, A. Mitchell, Methods in Yeast Genetics, Cold Spring Harbor Laboratory Press, NY, 1994.

[19] B.S. Glick, L.A. Pon, Isolation of highly purified mitochondria from *Saccharomyces cerevisiae*, Methods in Enzymology 260 (1995) 213–223. http://dx.doi.org/10.1016/0076-6879(95)60139-2 8592446.

[20] K.H. Slekar, D.J. Kosman, V.C. Culotta, The yeast copper/zinc superoxide dismutase and the pentose phosphate pathway play overlapping roles in oxidative stress protection, Journal of Biological Chemistry 271 (1996) 28831–28836. http://dx.doi.org/10.1074/jbc.271.46.28831 8910528.

[21] I. Kos, J.S. Rebouças, G. DeFreitas-Silva, D. Salvemini, Z. Vujaskovic, M.W. Dewhirst, I. Spasojević, I. Batinić-Haberle, Lipophilicity of potent porphyrin-based antioxidants: comparison of ortho and meta isomers of Mn(III) N-alkylpyridylporphyrins, Free Radical Biology & Medicine 47 (2009) 72–78. http://dx.doi.org/10.1016/j.freeradbiomed.2009.04.002 19361553.

[22] J.M. De Freitas, A. Liba, R. Meneghini, J.S. Valentine, E.B. Gralla, Yeast lacking Cu−Zn superoxide dismutase show altered iron homeostasis. Role of oxidative stress in iron metabolism, Journal of Biological Chemistry 275 (2000) 11645–11649. http://dx.doi.org/10.1074/jbc.275.16.11645 10766782.

[23] C. Srinivasan, A. Liba, J.A. Imlay, J.S. Valentine, E.B. Gralla, Yeast lacking superoxide dismutase(s) show elevated levels of "free iron" as measured by whole cell electron paramagnetic resonance, Journal of Biological Chemistry 275 (2000) 29187–29192. http://dx.doi.org/10.1074/jbc.M004239200 10882731.

[24] I. Dilova, C.Y. Chen, T. Powers, Mks1 in concert with TOR signaling negatively regulates RTG target gene expression in *S. cerevisiae*, Current Biology 12 (2002) 389–395. http://dx.doi.org/10.1016/S0960-9822(02)00677-2 11882290.

[25] Z. Liu, R.A. Butow, Mitochondrial retrograde signaling, Annual Review of Genetics 40 (2006) 159–185. http://dx.doi.org/10.1146/annurev.genet.40.110405.090613 16771627.

[26] L.T. Jensen, R.J. Sanchez, C. Srinivasan, J.S. Valentine, V.C. Culotta, Mutations in *Saccharomyces cerevisiae* iron–sulfur cluster assembly genes and oxidative stress relevant to Cu,Zn superoxide dismutase, Journal of Biological Chemistry 279 (2004) 29938–29943. http://dx.doi.org/10.1074/jbc.M402795200 15107423.

[27] E. Zyracka, R. Zadrag, S. Kozioł, A. Krzepiłko, G. Bartosz, T. Biliński, Yeast as a biosensor for antioxidants: simple growth tests employing a *Saccharomyces cerevisiae* mutant defective in superoxide dismutase, Acta Biochimica Polonica 52 (2005) 679–684 16175242.

[28] T. Weitner, I. Kos, H. Sheng, A. Tovmasyan, J.S. Rebouças, P. Fan, D.S. Warner, Z. Vujaskovic, I. Batinic-Haberle, I. Spasojevic, Comprehensive pharmacokinetic studies and oral bioavailability of two Mn porphyrin-based SOD mimics, MnTE-2-PyP5+ and MnTnHex-2-PyP5+, Free Radical Biology & Medicine 58 (2013) 73–80. http://dx.doi.org/10.1016/j.freeradbiomed.2013.01.006 23328731.

[29] Y. Zhao, S. Miriyala, L. Miao, M. Mitov, D. Schnell, S.K. Dhar, J. Cai, J.B. Klein, R. Sultana, D.A. Butterfield, M. Vore, I. Batinic-Haberle, S. Bondada, D.K. St Clair, Redox proteomic identification of HNE-bound mitochondrial proteins in cardiac tissues reveals a systemic effect on energy metabolism after doxorubicin treatment, Free Radical Biology & Medicine 72 (2014) 55–65. http://dx.doi.org/10.1016/j.freeradbiomed.2014.03.001 24632380.

[30] A.K. Holley, Y. Xu, T. Noel, V. Bakthavatchalu, I. Batinic-Haberle, D.K. St Clair, Manganese superoxide dismutase-mediated inside-out signaling in HaCaT human keratinocytes and SKH-1 mouse skin, Antioxidants & Redox Signaling 20 (2014) 2347–2360. http://dx.doi.org/10.1089/ars.2013.5204.